

Various regimes of flux motion in $\text{Bi}_{1-x}\text{Sr}_x\text{CaCu}_2\text{O}_{8+y}$ single crystals

Weimin Chen, J.P. Franck, and J. Jung

Department of Physics, University of Alberta, Edmonton, Canada T6G 2J1

Four regimes of vortex motion were identified in the magnetoresistance of $\text{Bi}_{1-x}\text{Sr}_x\text{CaCu}_2\text{O}_{8+y}$ single crystals: (1) thermally activated flux flow (TAFF) in samples with surface defects caused by thermal annealing; (2) TAFF-like plastic motion of highly entangled vortex liquid at low temperatures, with $U_{p1} \propto (1 - T/T_c)^{1/2}$; (3) pure free flux flow above the region of (2) in clean and optimally doped samples; or, in its place, (4) a combination of (2) and (3). This analysis gives an overall picture of flux motion in Bicuapates.

The layered structure of high- T_c cuprates causes intrinsic pinning even in the vortex liquid state. According to Vinokur et al. [1], such pinning arises from the plastic creep due to flux entanglement. The highly viscous flux motion gives rise to an activation-type resistivity, $\rho_{p1} = \rho_0 \exp(U_{p1}/T)$, with $U_{p1} \propto (1 - T/T_c)^{1/2}$. This pinned liquid model had been confirmed in recent experimental studies [2]. Another interesting phenomenon is free flux flow, as described by the classical Bardeen-Stephen model [3], which occurs when the pinning barrier is suppressed. Plastic creep and free flux flow are generally difficult to verify in experiment, because they can be easily replaced by defect pinning effects. Free flux flow (FFF) was only observed in clean YBCO samples [4], or under high driving forces by using current pulses [5]. For Bicuapates, intrinsic pinning is weaker due to its higher anisotropy, and is thus more difficult to investigate. In the present work, we report different regimes in flux motion under various pinning circumstances, by measuring the magnetoresistance of $\text{Bi}_{1-x}\text{Sr}_x\text{CaCu}_2\text{O}_8$ single crystals.

1. Pinning by surface defects In annealed samples, thermally activated flux flow (TAFF) resistance (with T -independent barrier) was consistently observed down to the lowest T . Before annealing, on the other hand, a crossover behavior frequently occurred: below some crossover T_x , plastic creep was identified in agreement with the pinned liquid scenario; Above T_x it crossovers to either pure free flux flow or a combination of FFF and TAFF. This clear difference between as-

grown and annealed samples is connected to the effect of annealing. Scanning microscopy imaging revealed that the atomic-scale smooth surfaces of as-grown samples could be damaged by thermal annealing (450°C for 4h). Partial evaporation of material results a mesh of sub- μm -sized pits on the sample surfaces. Obviously, such defects can effectively cause pinning to give rise to the TAFF behavior over wide temperature ranges, even when the bulk pinning is absent.

2. Pinning in vortex liquid Figure 1 shows a typical set of resistance data for fields applied along the c -axis of an as-grown Bi-2212 sample ($T_c = 76\text{ K}$). The crossover in flux motion is evident. Similar phenomenon is also clear in other as-grown samples, one of which is presented in Fig. 2. We tried to fit the tail below the crossover temperature to the pinned-liquid model [1]: $\rho_{p1} = \rho_0 \exp(U_{p1}/T)$, with $U_{p1} = \frac{1}{2} a (1 - T/T_c) = \frac{1}{2} \phi_L(0)^2 U_0 (1 - T/T_c)$, where $a = (\phi_0/H)^{1/2}$ is the inter-vortex spacing. The result is given by the solid lines in Fig. 1, which shows satisfactory agreement. The extracted field dependence of U_0 from Figs. 1 and 2 is plotted in the inset of Fig. 2. At high fields, U_0 also follows the $1/H$ dependence as predicted (the straight line of $-1/2$ slope). Similar behavior and crossover at low fields were reported for Bi-2212 [6] and 2223 [7].

3. Free flux flow Above the crossover temperature, flux lines become disentangled and the pinning vanishes ($U < k_B T$). In this regime, free flux flow is thus expected if there exists no defect pinning. We tried to fit the resistance to

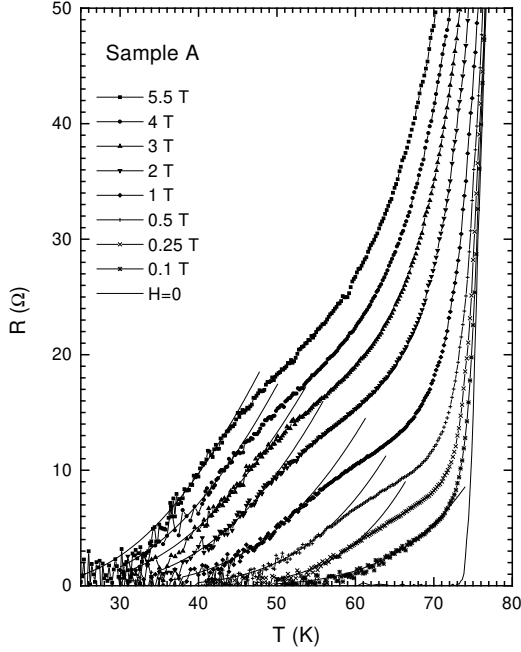


Figure 1. Resistance of an as-grown Bi-2212 sample. Crossover in flux motion is evident as T increases. The solid lines are fittings to plastic-flow model: $R_{pl} / \exp[U_{pl}(H; T) = T]$.

the Bardeen-Stephen model: $R_f = R_N H / H_{c2}$, where R_N is the normal-state extrapolated resistance and $H_{c2} = (T_c - T)$. One of the results is as shown in Fig. 2 (solid lines). The fitting is impressive over a very wide temperature range (51 to 78 K for $H = 5.5$ T, $T_c = 85$ K). The value of β is about 0.8 to 1.4 T/K, increasing with field. This result closely agrees with literature data (0.75 T/K) [8].

4. An intermediate situation involves combined contributions of both FFF and TAFF, as revealed by resistivity of YBCO [9]. The total resistivity is expressed as [10]: $1 = 1_{fff} + 1_{taff}$. A preliminary fitting of our data to this scheme seems to explain the resistance above the crossover T in Fig. 1.

In summary, we emphasize the pinning effect of the surface defects caused by thermal annealing, which results in activation-type flux flow even when the bulk pinning is absent. In clean samples, vortex motion was analyzed in the schemes

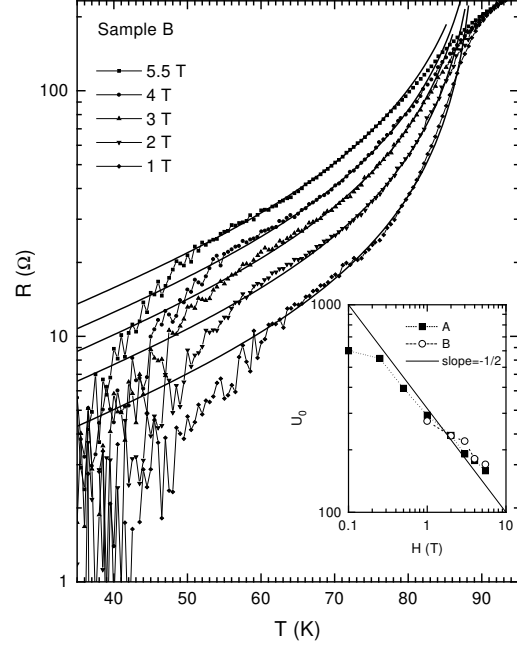


Figure 2. Crossover behavior and free flux flowing (solid lines). Inset: field dependence of U_0 (see text) for Samples A and B, showing an approximate $1 = H$ relation (straight line).

of pinned liquid (plastic flow) and free flux flow.

REFERENCES

1. V. M. Vinokur et al, Phys. Rev. Lett. 65 (1990) 259.
2. S. N. Gordeev et al, preprint.
3. J. Bardeen and M. J. Stephen, Phys. Rev. 140 (1965) A1197.
4. K. K. Krishana et al, Phys. Rev. Lett. 82 (1999) 5108.
5. N. B. Kunchur et al, Phys. Rev. Lett. 70 (1993) 998.
6. L. M. Ju et al, Phys. Rev. B 57 (1998) 3151.
7. H. Yamasaki et al, Phys. Rev. B 49 (1994) 6913.
8. T. T. M. Palstra et al, Phys. Rev. B 38 (1988) 5102.
9. M. G. Jura et al, Phys. Rev. B 45 (1992) 7387.
10. G. B. Latter et al, Rev. Mod. Phys. 66 (1994) 1125.